Figure S1. Related to Figures 1 and 2

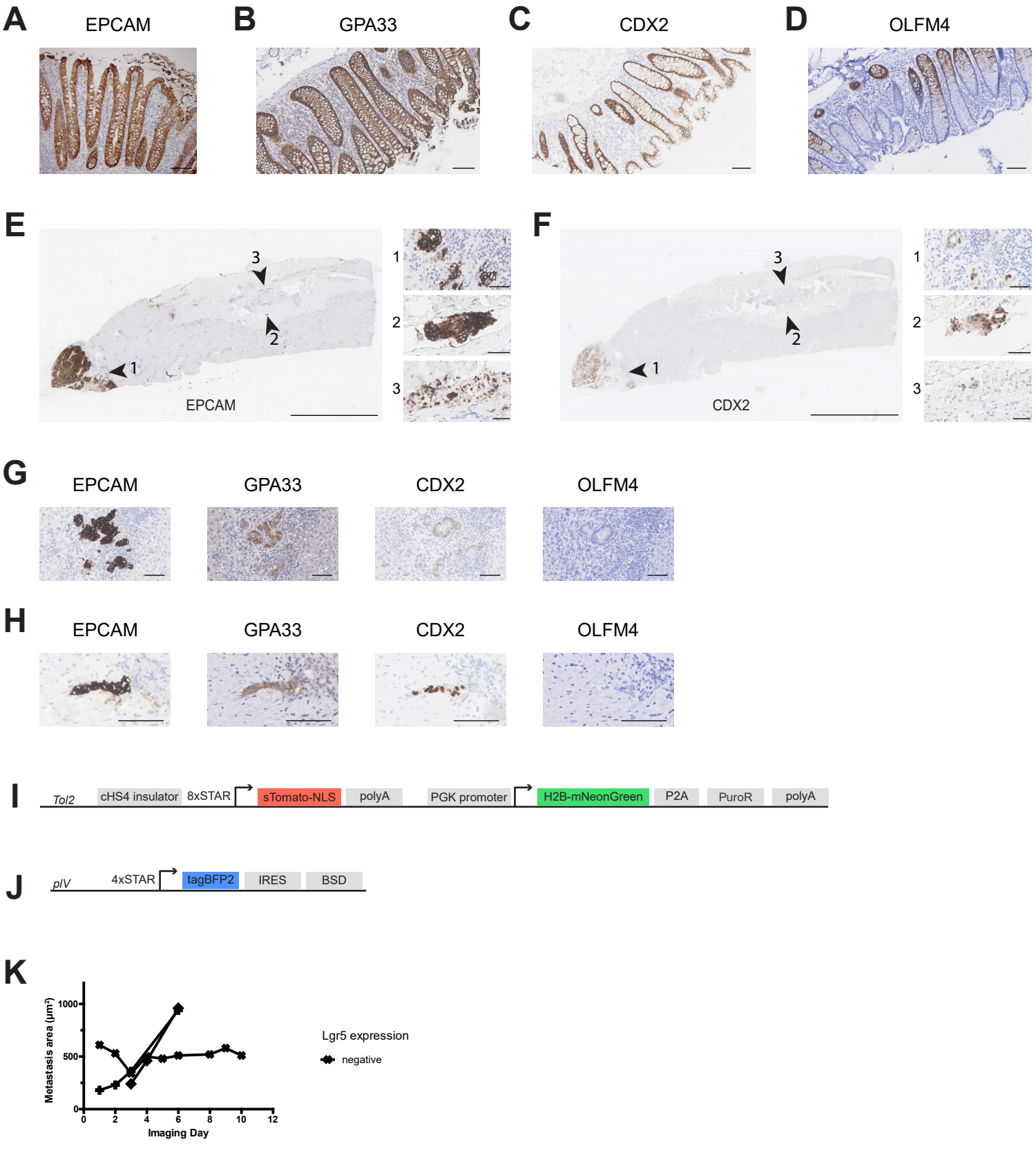

Figure S1: Related to Figures 1 and 2

(A-D) Representative images of antibody stainings on human colon sections for (A) EPCAM, (B) GPA33, (C) CDX2, and (D) OLFM4. Scale bars, 100 µm.

(E-F) Patient-derived liver tissue strip stained for (E) EPCAM and (F) CDX2 to identify cells of colonic origin. The positions of micrometastases (positive for EPCAM, CDX2, and GPA33) are indicated by arrowheads. Scale bars, 5 mm (in close ups, 50 µm). Related to Figure 1B.

(G-H) Two examples of micrometastases identified by stainings for EPCAM, GPA33, and CDX2. Micrometastases are completely devoid of the SC marker OLFM4. Scale bars, 100 µm.

(I) Schematic of STAR reporter design suitable for Tol2 transposon-based integration. Having 8 repeats of an ASCL2 motif (8xSTAR) upfront, transcriptional activity of ASCL2 is reported by nuclear expression of sTomato. Additionally, ubiquitous expression of H2B fused to mNeonGreen is driven by an independent, ubiquitously active PGK promoter. Other elements: insulator sequence preventing 5' methylation (cHS4 insulator), polyadenylation signal (polyA), 2A self-cleavage peptide (P2A), puromycin selection cassette (puroR). This STAR is a derivative of the previously published STAR (Figure S1J) (40).

(J) Design of the STAR reporter as previously published (40). 4xSTAR indicating 4 repeats of the ASCL2 binding site. Other elements: Internal ribosome entry site (IRES) and blasticidin selection cassette (BSD).

(K) Traces of individual metastases that are devoid of Lgr5 expression during the whole course of IVM, depicting the size of the lesions over time. This data is a subset of the data depicted in Figure 2E but with a different scale.

Figure S2. Related to Figure 3

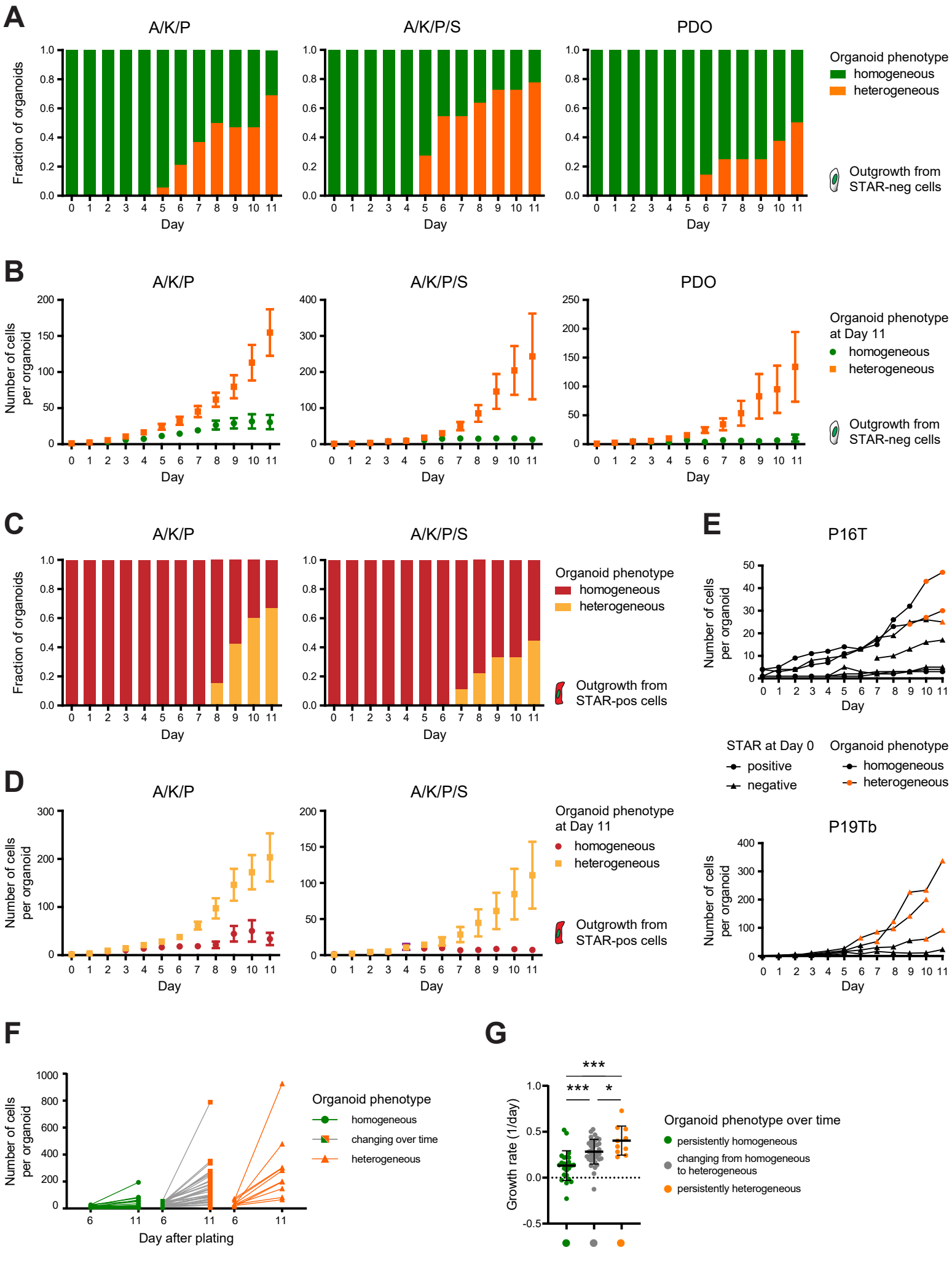

Figure S2: Related to Figure 3

Quantification of the outgrowth behaviour of human CRC organoid lines over time with respect to cellular composition. (A-E) The data is stratified by organoid line. Engineered CRC with *APC*$^{KO/KO}$/*KRAS*$^{G12D/-}$/*TP53*$^{KO/KO}$ (A/K/P); engineered, metastatic A/K/P with additional *SMAD4*$^{KO/KO}$ (A/K/P/S); PDOs P16T and P19Tb pooled (PDO). The pooled data of all lines is presented in Figure 3.

A. Graph representing the fraction of organoid phenotypes (homogeneous versus heterogeneous) per indicated time point during the outgrowth of STAR^{-} CRC cells.
B. Number of cells per organoid over time, stratified by organoid phenotype at the final day of tracking. Graph represents the mean size + SEM for the outgrowth of STAR^{-} cells.
C. Graph representing the fraction of organoid phenotypes (homogeneous versus heterogeneous) per indicated time point during the outgrowth of STAR^{+} CRC cells.
D. Number of cells per organoid over time, stratified by organoid phenotype at the final day of tracking. Graph represents the mean size + SEM for the outgrowth of STAR^{+} cells.
E. Single PDO outgrowth traces over time depicting the organoid phenotypes to be either homogeneous organoids (black) or heterogeneous (orange). Outgrowth of single STAR^{-} (triangle) or STAR^{+} cells (dots). PDOs: P16T (top) and P19Tb (bottom).
F. Paired data of individual organoids at Day 6 and 11 of culturing. Number of cells per organoid is plotted and the organoid phenotype is indicated by colour for each time point to be either homogeneous (green) or heterogeneous (orange).
G. Computed growth rate of individual organoids plotted in panel F. The growth rate distributions of the three phenotype groups was compared with a two-tailed Student's t-test (p-value < 0.0001 for comparisons left vs. middle and left vs. right and 0.0002 for comparison middle vs right).

Figure S3. Related to Figure 3

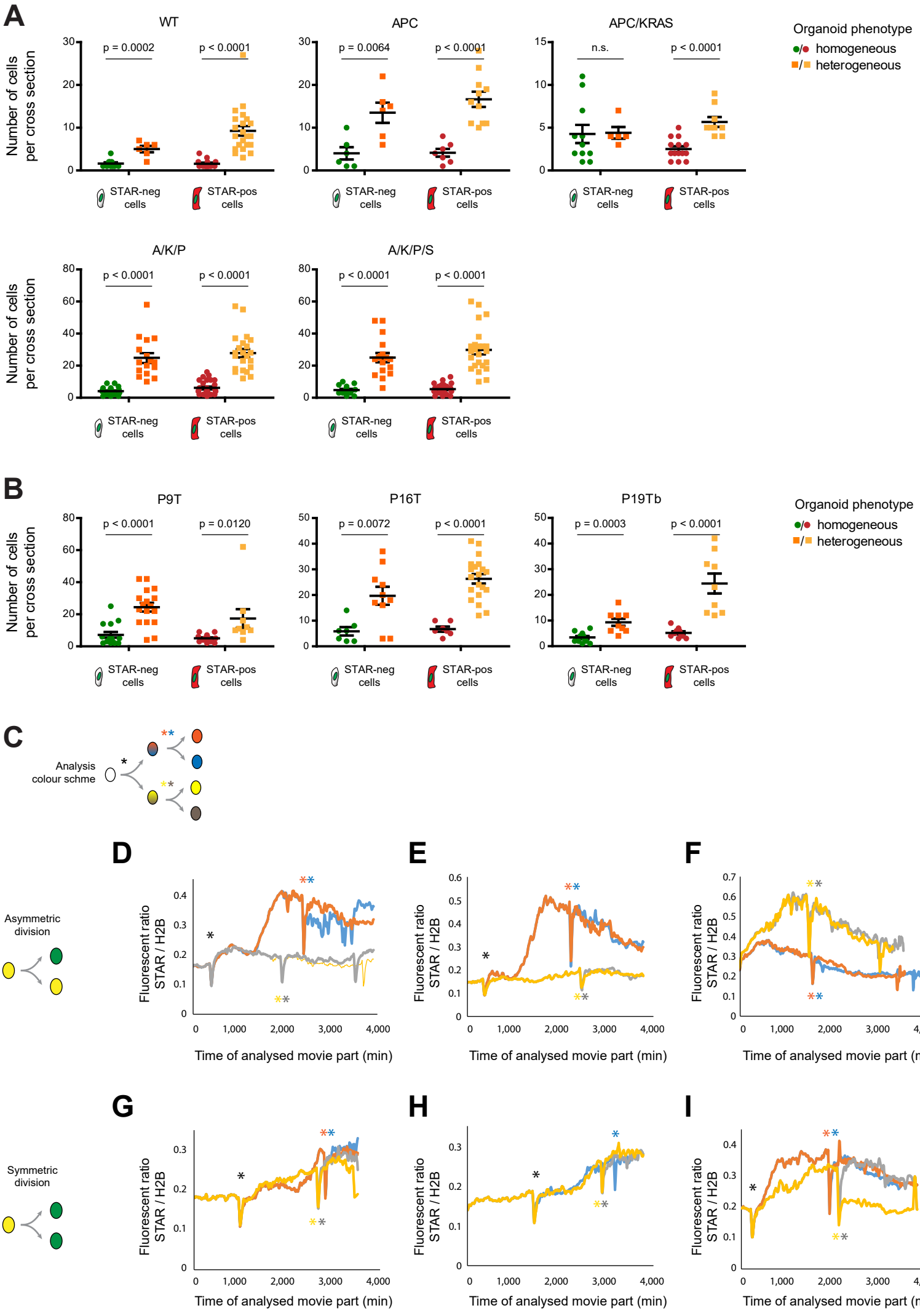

Figure S3: Related to Figure 3

(A-B) Organoid size after 10 days of culturing is depicted as the number of nuclei per organoid cross section at its widest position. Single $STAR^-$/$STAR^+$ cells grew either into homogeneous structures (green/red) or into heterogeneous structures (orange/yellow). Organoid size stratified by phenotype was compared using a two-tailed Student's t-test.

A. Data generated with human colon WT and engineered human CRC lines with the following mutations: loss of *APC* (APC or A), *TP53* (P), *SMAD4* (S), and oncogenic $KRAS^{G12D/-}$ (KRAS or K).
B. Data generated with PDOs P9T, P16T and P19Tb.

(C-I) Analysis of early cell plasticity events during PDO outgrowth starting at preceding mitosis (black asterisk) up until 1-2 mitoses later (coloured asterisks). Ratio intensities of measured nuclear STAR over H2B signal are plotted for the individual cells. Mitoses coincide with dips in ratio plot due to dilution of STAR signal during nuclear envelope breakdown. (C) Schematic of colour/lineage assignment. (D-F) and (G-I) show plasticity events with asymmetric and symmetric divisions in division round 1, respectively.

Figure S4. Related to Figure 4

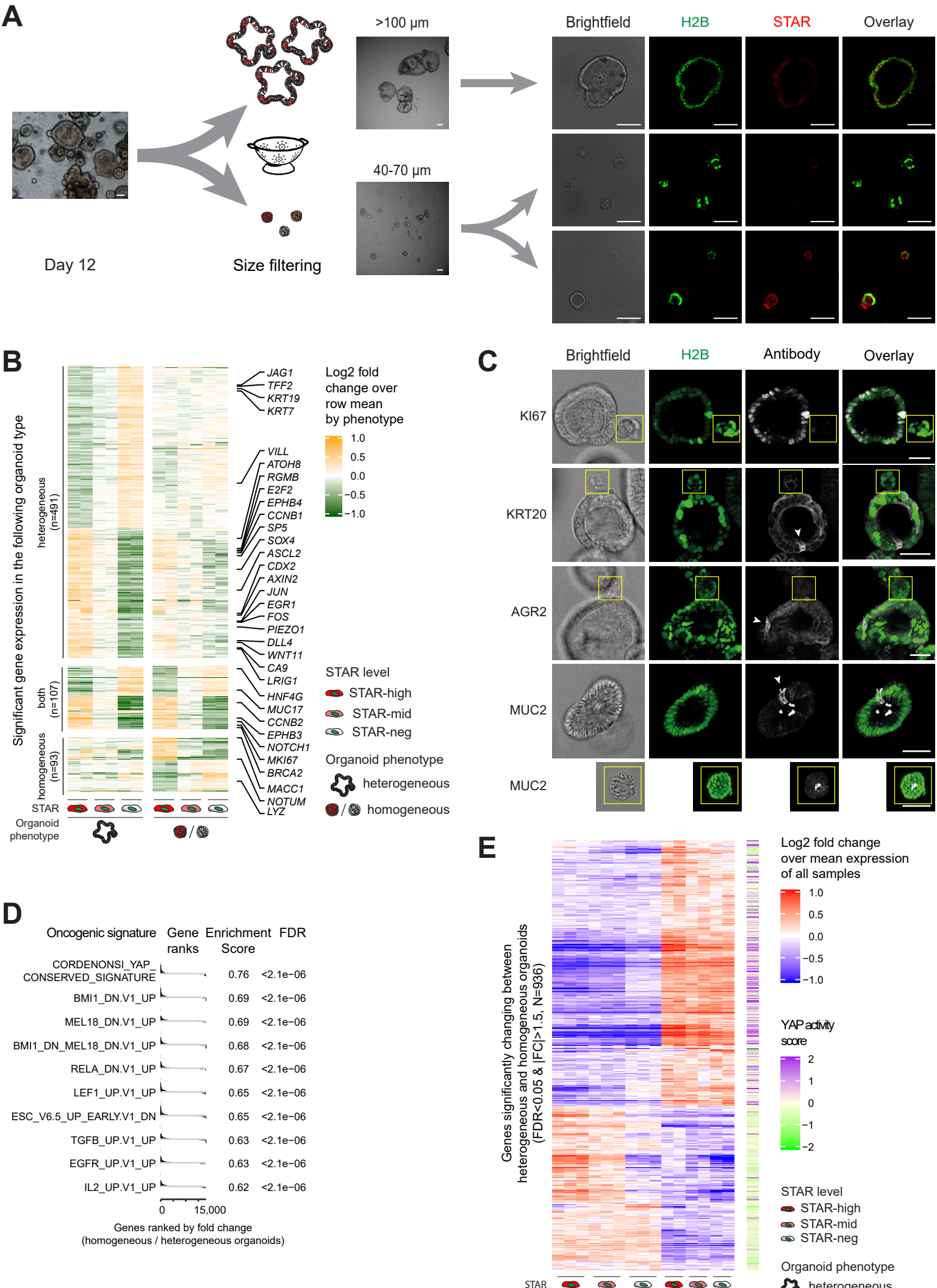

Figure S4: Related to Figures 4

A. Representative images of organoids prior to and after size filtering with STAR-neg and STAR-pos micro-organoids (40-70 µm, centre and bottom row, respectively). H2B chromatin-tag (green), STAR (red). Scale bars, 100 µm.
B. Heatmap depicting genes being differentially expressed for at least one comparison between STAR-high, STAR-mid, and STAR-neg samples with FDR < 0.01. Genes are grouped to be dynamically expressed in heterogeneous (top), homogeneous (bottom), or both organoid phenotypes (mid). Gene expression was normalised to the row mean of samples of the respective organoid phenotype. Equal numbers of replicates (N=2) were considered for each biological condition in this analysis.
C. Representative images of small and large A/K/P/S or P16T organoids stained for the proliferation marker KI67 and differentiation markers KRT20, AGR2, and MUC2. Micro-organoids are outlined by a yellow box. Cells positive for the differentiation markers are indicated with an arrowhead. Scale bars, 50 µm.
D. Comparison of the homogeneous organoid signature (gene expression of homogeneous over heterogeneous organoids, ranked by fold change) to the oncogenic signatures of Molecular Signature Database (MSigDB). Enrichment score and FDR is depicted for the top 10 hits. Ranking starts with genes upregulated in homogeneous micro-organoids (left).
E. Heatmap showing all differentially expressed genes between homogeneous and heterogeneous organoids (fold change (FC) > 1.5, FDR < 0.05) to which a YAP score could be assigned.

Figure S5. Related to Figures 4-6

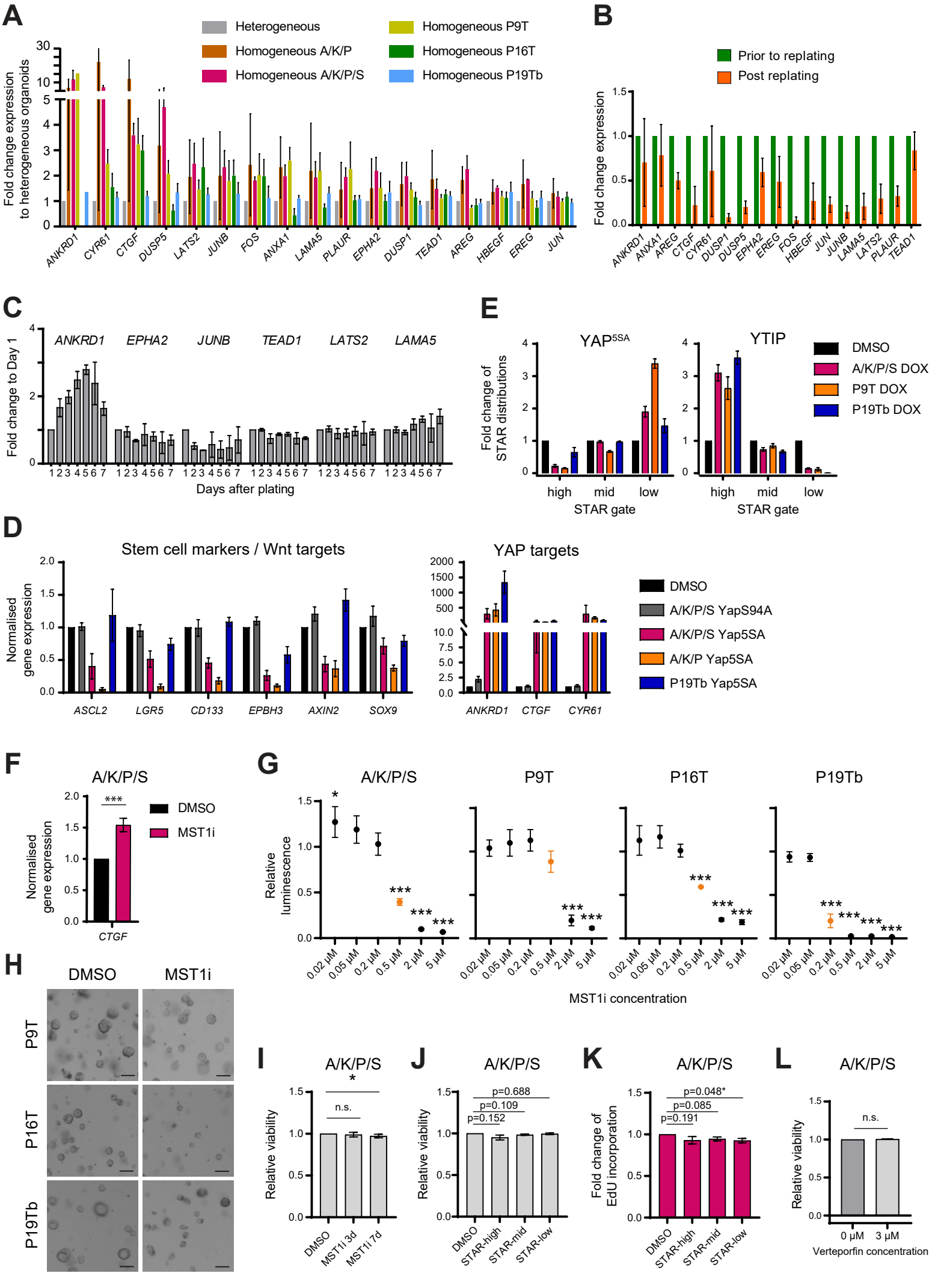

Figure S5: Related to Figures 4-6

A. Expression pattern of *micro-organoid associated genes* across engineered and patient-derived CRC organoid lines after size filtering for small (homogeneous) and large (heterogeneous) organoids. Gene expression, assessed by qPCR, is normalised to heterogeneous organoids. Data shows mean + SEM of 2-4 independent experiments. Related to Figure 4I.
B. Gene expression of A/K/P/S micro-organoids isolated from a 12 day culture with (orange) or without (green) replating intact organoids into new Matrigel and harvesting after another 16h. Mean expression + SEM of three independent experiments is indicated.
C. Gene expression over time in A/K/P/S organoids growing from single cells for a selection of genes being upregulated in micro-organoids. Gene expression is normalised to Day 1. Data shows mean + SEM of two independent experiments.
D. Gene expression of YAP targets and SC markers / Wnt targets upon overexpression of either constitutively active YAP^{5SA} or a TEAD-binding-dead mutant YAP^{S94A}. qPCR data was normalised to housekeeping genes and data is represented as fold change to DMSO treated samples (mean + SEM of 3-4 independent experiments).
E. Flow analysis of STAR levels in 3 different CRC organoid lines upon perturbation of YAP activity via inducible overexpression (48 hrs) of the constitutively active YAP mutant YAP^{5SA} or the YAP mimetic YTIP. Inhibiting YAP activity skews cells towards high STAR levels, at the expense of cells with low to medium levels of SC activity. Conversely, stimulating YAP activity skews cells towards low STAR levels, at the expense of cells with high levels of SC activity. Analysis at Day 5 of outgrowth. Data represents the change for each STAR population compared to DMSO as mean + SEM.
F. Gene expression data of YAP targets in A/K/P/S organoids treated for 48h with 500 nM of the MST1/2 inhibitor XMU-MP-1. qPCR data was normalised to housekeeping genes and is represented as fold change to DMSO treated samples (mean + SEM of 4 independent experiments).
G. Relative viability of CRC organoids treated with a concentration range of the MST1/2 inhibitor for 7 days after plating single cells. CellTiter-Glo data is normalised to DMSO

control. The level of significance of the difference between MST1i-treated cells and the DMSO control was assessed using a two-tailed Student's t-test.

H. Representative images of CRC organoids after 7 days of MST1/2 inhibitor treatment (500 nM for P9T and P16T and 200 nM for P19Tb). Scale bars, 100 µm.

(I-L): Flow analysis of A/K/P/S organoids with respect to (I-J, L) viability and (K) EdU incorporation upon the following drug treatments: (I) 500 nM MST1/2 inhibitor was added for 3 or 7 days to single cells. (J-K) 500 nM MST1/2 inhibitor was added for 96 h to 10-day-old organoids. (L) 3 µM verteporfin was added for 48 h to single cells. Viability readout was assessed upon DAPI wash-in before flow analysis. EdU incorporation was assessed after addition of 500 nM EdU to the culture for the last 16 h. All data is normalised to the respective DMSO control and significance levels were assessed by two-tailed Student's t-test.

Figure S6. Related to Figure 7

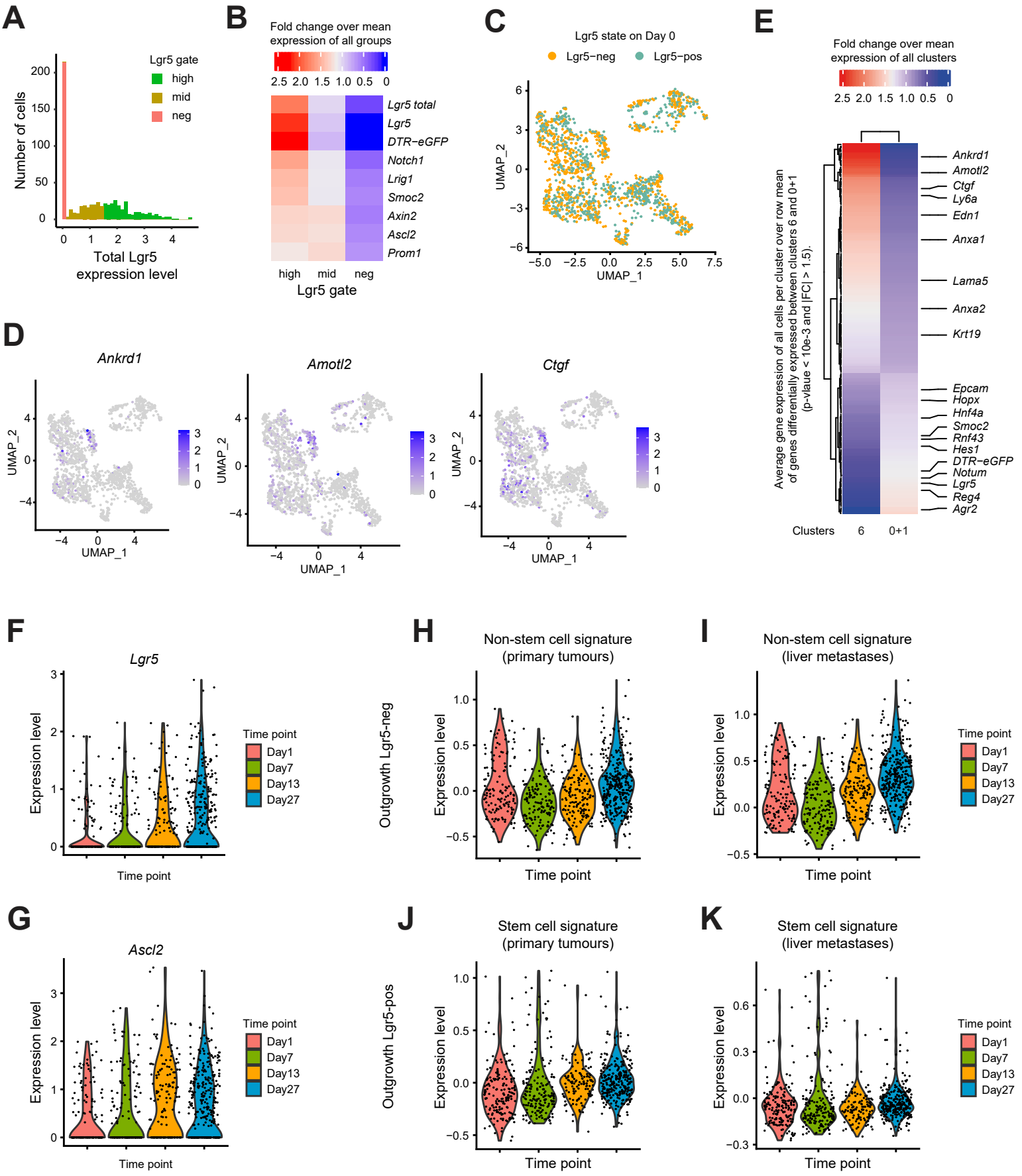

Figure S6: Related to Figure 7

A. Histogram of total Lgr5 expression computed as the sum of both alleles (WT and DTR-eGFP) after normalization of the data. Lgr5-high (green), -mid (orange), and –neg (red) subpopulations are determined by total expression level > 1.5 (37.5 % of all cells), < 1.5 but > 0 (27.5 % of all cells), zero (35.0 % of all cells).
B. Heatmap of selected SC markers and Wnt targets stratified by Lgr5 populations defined in (A). Data is represented as fold change over row mean for each gene.
C. UMAP of scRNA-seq data colour-coded by the Lgr5 state at the time of injection.
D. UMAP with colour-coded gene expression levels of the following Yap target genes: *Ankrd1*, *Amotl2*, and *Ctgf*.
E. Average gene expression for all differentially expressed genes between cluster 6 and clusters 0 and 1 (p-value < 10e-3 and |FC| > 1.5). Expression value is normalised by row mean and candidate genes are annotated.
F. Gene expression of *Lgr5* over time of all cells being $Lgr5^-$ at time of injection.
G. Gene expression of *Ascl2* over time of all cells being $Lgr5^-$ at time of injection.
H. Expression levels of signature of non-SCs over time for $Lgr5^-$ injected cells. Signature is based on cells growing in primary tumours (8).
I. Expression levels of signature of non-SCs over time for $Lgr5^-$ injected cells. Signature is based on cells growing in liver metastases (8).
J. Expression levels of SC signature over time for $Lgr5^+$ injected cells. Signature is based on cells growing in primary tumours (8).
K. Expression levels of SC signature over time for $Lgr5^+$ injected cells. Signature is based on cells growing in liver metastases (8).

Supplementary tables

Table S1: Characteristics of patients included for liver specimen collection. Related to Figure 1

Basic characteristics of CRC patients undergoing resection for liver metastases which were included for liver specimen collection and subsequent immunohistochemistry analysis for the presence of micro-metastases. Abbreviations: Mismatch repair (MMR), transarterial radioembolization (TARE), selective internal radiation therapy (SIRT), microsatellite stable (MMS), microsatellite instable (MSI), not detected (n.d.).

Table S2: Details on antibodies used in this study.

Table S3: Key features of micro-organoid genes. Related to Figures 4 and 5

Selection of genes upregulated in micro-organoids in RNAseq (Figure 4). Genes were selected due to a high YAP score and/or to a high fold change in expression between homogeneous and heterogeneous organoids (FC small / big). Selection of genes due to their YAP score was performed after filtering genes for (1) FDR size comparison < 0.001 (FDR Size), (2) YAP score > 1.5 (non-NA), and (3) mean expression of all samples > 9. Rank of genes after sorting final list by decreasing YAP score is indicated (Rank YAP Filtering). Selection of genes due to their expression fold change was performed after filtering genes for (1) FDR size comparison < 0.001, (2) expression fold change homogeneous / heterogeneous organoids > 3, and (3) mean expression of all samples > 9. Rank of genes after sorting final list by decreasing fold change is indicated (Rank FC Filtering). Forward and reverse primer sequences of each gene used in RT-qPCR experiments are indicated.

Video S1: Time-lapse microscopy of fragmented STAR organoids. Related to Figure 3

STAR organoids were fragmented into small structures and imaged for 7-8 days on a lattice light-sheet microscope. H2B (green), STAR (red), overlay (yellow-orange)

Top left: STAR-neg P19Tb organoid structure developing heterogeneity over time. Scale bar, 35 µm.

Top right: Heterogeneous P19Tb STAR organoid is continuously dividing and maintaining heterogeneity. STAR intensity is first transiently downregulated, reminiscent of transient YAP activity repressing stemness early during outgrowth. STAR-high cells become more pronounced over time. Scale bar, 50 µm.

Bottom left: STAR-pos P19Tb organoid structure growing into a heterogeneous organoids after transient downregulation of STAR, reminiscent of transient YAP activity repressing stemness early during outgrowth. Scale bar, 35 µm.

Bottom right: Fragmented A/K/P/S organoid showing heterogeneous STAR levels at all times. Within this panel: (Centre) Small STAR-low structure grows into a heterogeneous organoid after transient downregulation of STAR. (Bottom left) STAR-high micro-organoid with limited proliferation and without development of heterogeneity (partially outside field of view). Scale bar, 50 µm.